Engineering wave localization in a fractal waveguide network

Biplab Pal, Pinaki Patra, Jyoti Prasad Saha, and Arunava Chakrabarti*
Department of Physics, University of Kalyani, Kalyani, West Bengal-741 235, India
(Received 5 October 2012; published 13 February 2013)

We present an exact analytical method of engineering the localization of classical waves in a fractal waveguide network. It is shown that a countable infinity of localized eigenmodes with a multitude of localization lengths can exist in a Vicsek fractal geometry built with diamond-shaped monomode waveguides as the "unit cells." The family of localized modes forms clusters of increasing size. The length scale at which the onset of localization for each mode takes place can be engineered at will, following a well-defined prescription developed within the framework of a real space renormalization group. The scheme leads to an exact evaluation of the wave vector for every such localized state, a task that is nontrivial, if not impossible for any random or deterministically disordered waveguide network.

DOI: 10.1103/PhysRevA.87.023814 PACS number(s): 42.25.Dd, 42.82.Et, 72.15.Rn

I. INTRODUCTION

Since its inception, the phenomenon of Anderson localization in a disordered lattice [1] has been found to be ubiquitous in diverse fields of condensed matter physics and materials science. While the popular domain of interest is related to electronic systems, where the quantum interference plays a pivotal role in localizing electronic eigenstates in the presence of disorder [2–8], the effect is by no means confined to electrons and extends over a variety of phenomena ranging from spin freezing in one-dimensional semiconductors [9], localization in optical lattices [10–12], or the localization of matter waves (cold atoms forming Bose-Einstein condensates) [13,14], to name a few. Incidentally, the latter has recently been observed experimentally in one-dimensional matter waveguides where the random potential is generated by laser speckles [15].

In 1984 John [16] pointed out that the idea of localization goes far beyond the electronic systems and is actually a general phenomenon common to any wave propagation in systems with disorder. Anderson [17] followed with a seminal paper considering the idea of localization of classical waves, in an attempt to work out the theory of white paints. The field has gathered momentum in the last couple of decades and a considerable volume of literature related to the localization of classical waves, particularly light waves, ultrasound waves, and microwaves, is now in existence [18–26].

The study of localization of light in disordered media has been patronized by the discovery of the photonic band gap (PBG) materials [27–29]. These systems exhibit gaps in the frequency spectrum in which the propagation of waves is forbidden. This has important implications in both fundamental science and technological applications.

Photonic gaps, apart from materials with a large dielectric constant, can also be observed in waveguide networks, as proposed by several groups over the past years [30–38]. Anderson localized eigenmodes are observed inside the photonic gaps and excellent agreement between theory and experiments has been obtained [30]. The network models are able to localize a propagating wave by virtue of the geometrical arrangement of the waveguide segments. Of particular interest are a wide variety of models based on waveguide networks designed following a deterministic fractal geometry [34–38], where the gaps result from the typical topology exhibited by the hierarchical arrangement of the waveguide segments. The present communication also deals with a hierarchically designed (fractal geometry) waveguide network, but addresses a deeper fundamental question regarding wave localization in such systems, as explained below.

Fractals or hierarchical geometries in general cause an excitation to localize [39–42]. The energy spectrum turns out to be singular continuous [39], with a gap in the vicinity of every energy. Nevertheless, there can be a countable infinity of *extended* eigenfunctions with high (or even, perfect) transmittivity, even though there is no translational order in such systems. Once again, this is true for electrons [43–49], and classical waves as well [35,36]. A curious point, apparently gone unnoticed or unappreciated so far, is that, while a precise determination of the eigenvalues corresponding to the extended eigenmodes is possible in the above cases of hierarchically grown fractal networks, the task seems to be practically impossible when it comes to an exact evaluation of eigenvalues of the localized modes in such hierarchical systems in their *thermodynamic limits*. Direct diagonalization of the Hamiltonian (in the electronic case) or an exact numerical solution of the wave equation doesn't help, as the overall character of the spectrum in all the cases is highly fragmented, and the eigenvalues obtained from a finite sized network are likely to *slip away* from the spectrum once we go over to a higher generation. This problem has recently been addressed in the context of electron localization in fractal space [50], and we carry forward the central idea floated in Ref. [50] to evaluate the *exact* wavelengths (wave vectors) of the waves that can be localized *at will* in a properly designed hierarchical single-channel network.

We design a Vicsek fractal network [51] consisting of *diamond*-shaped loops, each arm of which mimics a single-mode linear waveguide (see Fig. 1). While examination of the localized mode eigenvalues and the nature of localization are indeed the major factors motivating this work, other interests in such a study are related to the general spectral character and classical wave transport in these systems. As one can easily appreciate, the geometry of a diamond-Vicsek network

*arunava_chakrabarti@yahoo.co.in

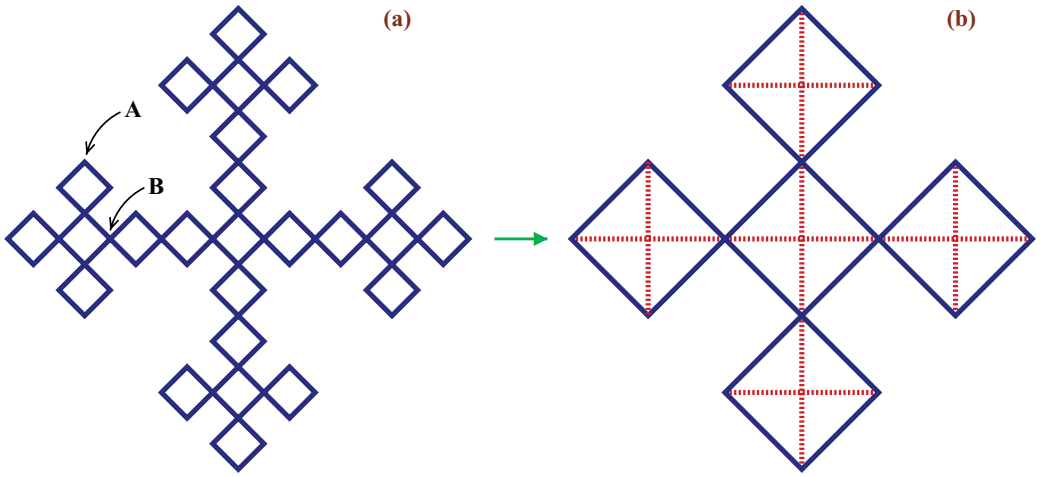

FIG. 1. (Color online) (a) Schematic view of the second generation of an infinite diamond-Vicsek waveguide network. The vertices at the junction of two waveguides are labeled as "*A*" in the text, while those in the bulk (at the crossing of four waveguides) are labeled as "*B*." (b) Renormalized version of panel (a) with the dotted lines indicating the diagonal "hopping" which is generated due to renormalization.

provides an interesting culmination of the "open" character of a typical Vicsek pattern and closed loops at shorter scales of length. This is in marked contrast to the much-studied Sierpinski gasket waveguide network [34], which is a closed structure, or to the other deterministic waveguide networks [36,37]. The presence of the loops generates the possibility of an effectively long-ranged propagation of waves between the various vertices, and its effect on the localization or delocalization of waves is worth studying.

We find interesting results. For an infinite hierarchical geometry, such as that presented above, a countable infinity of eigenmodes with a multitude of localization lengths can be *precisely detected*. One can work out an exact mathematical prescription to specify the length scale at which the onset of localization begins. The localization can, in principle, be *delayed* (staggered) in position space and the corresponding wave vectors (or wavelengths) can be exactly evaluated following the same prescription based on a real space renormalization group (RSRG) decimation method [52]. In addition, it is shown that for a given set of parameters, the center of the spectrum corresponds to a perfectly extended eigenmode, with the parameters describing the system exhibiting a fixed point behavior. This central extended mode is flanked on either side by localized wave functions with a hierarchy of localization lengths.

In what follows we describe the results. In Sec. II, the model and the mathematical method of handling the problem are presented. Section III discusses the results and their analyses, and in Sec. IV we draw our conclusions.

II. THE MODEL AND THE METHOD

A. The wave equation and its discretization

We have considered a waveguide network formed by waveguide segments having the same lengths arranged in a Vicsek fractal geometry [51]. Each segment has a single channel for wave propagation. The wave function ψ_{ij} between any two nodal points i and j satisfies the wave equation:

$$\frac{\partial^2\psi_{ij}(x)}{\partial x^2}+\frac{\omega^2}{c^2}\psi_{ij}(x)=0, \tag{1}$$

where ω is the frequency of the wave; c is the speed of wave propagation inside the material (waveguide) and is related to the speed of light in vacuum c_0 by the relation $c=c_0/\sqrt{\varepsilon}$, ε being the dielectric constant of the medium; and x is the distance measured from the ith node. The above equation has a solution of the form [53,54]

$$\psi_{ij}(x)=\psi_i\frac{\sin[k(\ell_{ij}-x)]}{\sin(k\ell_{ij})}+\psi_j\frac{\sin(kx)}{\sin(k\ell_{ij})}, \tag{2}$$

where $k=\omega/c=\omega\sqrt{\varepsilon}/c_0$ is the value of the wave vector inside the dielectric medium (waveguide), ℓ_{ij} is the length of the segment between the nodes i and j, and ψ_i and ψ_j are the values of the wave function at the ith and jth nodes, respectively. The flux conservation condition,

$$\sum_j\left[\frac{\partial}{\partial x}\psi_{ij}(x)\right]_{x=0}=0, \tag{3}$$

where the summation j is over all the nodes linked directly to i, leads to a discretized version of Eq. (1) [54], viz.,

$$-\psi_i\sum_j\cot\theta_{ij}+\sum_j\psi_j/\sin\theta_{ij}=0, \tag{4}$$

where $\theta_{ij}=k\ell_{ij}=ka$, a being the constant length of a waveguide, as considered in all the calculations which follow. Equation (4) resembles a tight-binding difference equation depicting the propagation of noninteracting electrons in a lattice, viz.,

$$(E-\epsilon_i)\psi_i=\sum_j t_{ij}\psi_j, \tag{5}$$

with the "electron energy" E and an "on-site potential," ϵ_i. $t_{ij}=1/\sin\theta_{ij}$ plays the role of a "hopping (overlap) integral" between the ith node and its neighboring nodes j. We exploit

this resemblance to investigate the localization aspects of classical waves. It is easy to see that, on replacing ka by $\pi - ka$, Eq. (5) can be recast with just t_{ij} being replaced by $-t_{ij}$. This does not change the spectrum or the nature of eigenstates in any way.

We have chosen to set, quite arbitrarily, $E = 2\cos ka$, so that $\epsilon_i = 2\cos ka + \sum_j \cot\theta_{ij}$. This does not affect the final results in any way. As seen in Fig. 1, the Vicsek waveguide network has two types of nodal points, viz., type A (having two neighboring nodal points) and type B (having four neighboring nodal points). Accordingly, in the equivalent wave propagation problem the on-site potentials should be assigned two values, viz., $\epsilon_A = 2\cos ka + 2\cot ka$ and $\epsilon_B = 2\cos ka + 4\cot ka$, respectively. The overlap integral along an arm of the waveguide is $t = 1/\sin ka$ and represents the overlap only between the nearest-neighbor vertices along an edge.

Now we come to an important point. There is no second-neighbor tunneling of the wave to begin with. However, the decimation of a subset of nodes will generate an additional overlap between the opposite vertices of a basic diamond plaquette in the rescaled version of the original network [see dotted lines in Fig. 1(b)]. To account for this, we define an *additional hopping* across the diagonals of a diamond plaquette, call it $t_{ij} = \lambda$, and set $\lambda = 0$ at the beginning. It is to be appreciated that, unlike the term $t = 1/\sin ka$, one should not look for any initial expression of λ. It is simply zero and the generation of this *additional hopping* is a result of the rescaling of the network only. The role of λ under successive RSRG steps is going to be important in observing any localization or extendedness of waveguide modes, as explained later.

We now proceed to describe the physics of wave propagation in such a fractal geometry by exploiting this exact analogy with the corresponding electronic problem.

B. The RSRG scheme

A renormalized version of the fractal network is easily obtained by decimating a subset of vertices from the original geometry. This implies one has to eliminate a subset of the wave amplitudes from the difference equations (5) in terms of the surviving vertices [see Fig. 1(b)]. This results in the following set of recursion relations for the system parameters, viz., on-site potentials,

$$\begin{aligned}
\epsilon_A' &= \epsilon_A + \left[\frac{2t^2}{E-\epsilon_A-\lambda} + \frac{\left(\lambda + \frac{2t^2}{E-\epsilon_A-\lambda}\right)^2\left((E-\epsilon_B) - \frac{2t^2}{E-\epsilon_A-\lambda} - \xi\right)}{\left((E-\epsilon_B) - \frac{2t^2}{E-\epsilon_A-\lambda} - \xi\right)^2 - \left(\lambda+\xi\right)^2}\right], \\
\epsilon_B' &= \epsilon_B + 2\left[\frac{2t^2}{E-\epsilon_A-\lambda} + \frac{\left(\lambda + \frac{2t^2}{E-\epsilon_A-\lambda}\right)^2\left((E-\epsilon_B) - \frac{2t^2}{E-\epsilon_A-\lambda} - \xi\right)}{\left((E-\epsilon_B) - \frac{2t^2}{E-\epsilon_A-\lambda} - \xi\right)^2 - (\lambda+\xi)^2}\right],
\end{aligned} \tag{6}$$

and the hopping (overlap) integrals,

$$\begin{aligned}
t' &= \frac{t[\lambda(E-\epsilon_A-\lambda)+2t^2]^2}{[E^2-(\epsilon_A+\epsilon_B)(E-\lambda)-2E\lambda+\lambda^2-2t^2+\epsilon_A\epsilon_B]^2 - 4t^2(E-\epsilon_A-\lambda)^2}, \\
\lambda' &= \frac{\left(\lambda + \frac{2t^2}{E-\epsilon_A-\lambda}\right)^2(\lambda+\xi)}{\left[(E-\epsilon_B) - \frac{2t^2}{E-\epsilon_A-\lambda} - \xi\right]^2 - (\lambda+\xi)^2},
\end{aligned} \tag{7}$$

where $\xi = 2t^2(E-\epsilon_A-\lambda)/\Delta$, with $\Delta = (E-\epsilon_A-\lambda)(E-\epsilon_B-\lambda) - 2t^2$, and $\lambda = 0$ at the beginning.

The scaling generates an effective second-neighbor hopping (overlap) λ', as pointed out in Sec. II A, and is obvious from the above set of recursion relations and Fig. 1(b). The rescaled network [Fig. 1(b)] represents an effective waveguide network where waveguide segments connect the vertices of a diamond plaquette along the edges as well as along the diagonals. The latter has a length different from the edges and hence λ' differs from t'. This is again equivalent to an electronic problem with first- and second-neighbor hopping integrals t' and λ', respectively [50], and forgetting about the classical wave altogether, the localization properties of the eigenmodes can now be studied via an evolution of these effective overlap integrals under successive RSRG steps, beginning at the stage depicted in Fig. 1(b). The parameters ϵ_A, ϵ_B, t, and $\lambda(=0)$ obviously do not retain their simple forms of the initial (bare length scale) stage.

These recursion relations will now be used to obtain information about the local density of eigenmodes at specific sites of the system and about the localized or extended character of the modes, as discussed below.

III. RESULTS AND DISCUSSION

A. Local density of eigenmodes

As already stated, the exact mapping of the wave equation onto a discrete Schrödinger type equation allows us to extract information about the density of wave eigenmodes through a Green's function analysis [52]. We present in Fig. 2 the density of modes at a B vertex, which is given by

$$\rho^{(B)}(ka) = \lim_{\eta\to 0}\left\{-\frac{1}{\pi}\,\mathrm{Im}[G^{(B)}(ka+i\eta)]\right\}. \tag{8}$$

The distribution of eigenmodes, plotted within $ka < 0 < 2\pi$, shows clusters of nonzero values over a finite range of the

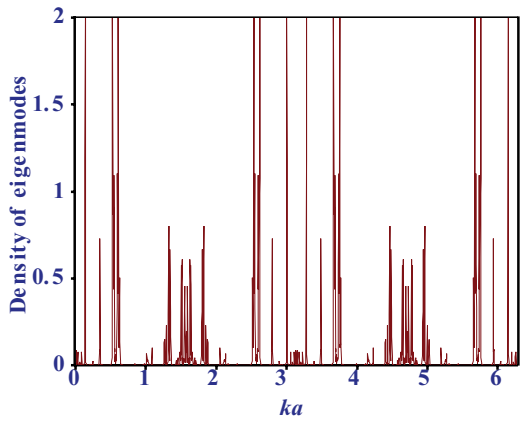

FIG. 2. (Color online) Local density of eigenmodes at a bulk B-type vertex of an infinite diamond-Vicsek waveguide network.

wave vector k and is found to be symmetric around $ka = \pi/2$. The fragmented Cantor-like character, the typical signature of a fractal spectrum, is apparent. An idea about the character of the eigenmodes can be obtained by observing the flow of t under successive RSRG iterations. In general, for an arbitrary value of ka, for which the density of modes is nonzero, $t^{(n)} \to 0$ as the number of iterations n increases, implying a localized character of the corresponding eigenmode [43,52]. However, for $ka = (2m+1)\pi/2$, both the first- and the second-neighbor hopping integrals t and λ remain nonzero for an indefinite number of iterations. In fact, we observe a one-cycle *fixed point* of the entire parameter space, viz., $\{\epsilon'_A,\epsilon'_B,t',\lambda'\} = \{\epsilon_A,\epsilon_B,t,\lambda\}$. The fact that t and λ remain finite at all stages of RSRG implies that there is a nonzero overlap between the wave amplitudes at all scales of length, and the corresponding mode is an extended one.

The neighborhood of $ka = (2m+1)\pi/2$ has been scanned minutely. The self-similarity of the spectrum is always seen with dense patches of eigenvalues clustered throughout the intervals. For many of these eigenvalues t and λ remain finite under successive decimation for a large number of steps. This indicates that every local *band center* at $ka = (2m+1)\pi/2$ is flanked either by extended modes or, at least, by eigenmodes with very large localization lengths.

B. Explicit construction of localized modes

The deterministic Vicsek fractal waveguide is self-similar at all scales of length. This feature allows us to explicitly construct a special distribution of wave functions by suitably exploiting the difference equations, Eq. (5). These "special" eigenmodes are localized and extend over clusters of single-channel waveguide segments of various sizes. The planar extent of such clusters depends on the eigenvalue corresponding to the localized mode and can be small or enormous, depending on the wavelength (or wave vector). The construction is similar to our recent work [50] on electronic states.

To elaborate, let us set

$$E = \epsilon_B(n) - 2\lambda(n), \tag{9}$$

where n refers to the stage of renormalization. This is, in general, a polynomial equation in E (and, hence, in k). The zeros of this equation will be the allowed wave vectors for the infinite system if, and only if, with them, one can satisfy Eq. (5) locally at every vertex of the network. This task can be accomplished by trying to draw a nontrivial distribution of amplitudes for a value of E (ka) obtained from Eq. (9) on the undecimated vertices of an n-step renormalized network and then trying to figure out the amplitude distribution on the original waveguide structure at the bare length scale. This can indeed be done, as we demonstrate in Fig. 3(a) for $n = 1$. For $n = 1$ Eq. (9) reduces to

$$\cos ka(2\cos 2ka - 1) = 0. \tag{10}$$

Roots of the above equation are $ka = \pm\pi/2$ and $ka = \pm\pi/6$. $ka = \pi/2$ (or, equivalently, $-\pi/2$) is of course, the extended mode. The root $ka = \pi/6$ leads to the construction of wave amplitudes as shown in Fig. 3. It is not difficult to extend the construction depicted in Fig. 3(a) even to a network of an arbitrarily large size, where the *end* vertices are not actually visible. We are still able to satisfy Eq. (5) locally at every vertex while drawing this distribution and, thus, $k = \pi/6a$ definitely belongs to the spectrum of the infinite system, a fact that has been cross-checked by evaluation of the local density of modes at the A and the B sites at this special value of k. We get a stable, finite value of the local density of modes which supports our argument above.

In Fig. 3(a) we show the distribution of amplitudes on the central cluster of an infinite diamond-Vicsek hierarchical network for $ka = \pi/6$. The deep red arms connect network vertices where the wave amplitudes are nonzero, and thus these arms are the brightest looking ones as far as the distribution of light intensity is concerned. The black lines represent waveguides which will appear completely dark, as the wave amplitudes at their vertices will have to be zero in order to satisfy Eq. (5). There will be arms connecting one vertex with a zero amplitude and another with a nonzero one. These are depicted by a lighter shade of red and will "glow" with less intensity compared to the deep red ones. The distribution of intensity in any arm (apart from the black ones) is by no means uniform. The colors just represent the fact that the intensity is nonzero. The significant observation is that clusters of nonzero amplitude span over a finite distance, but ultimately get "decoupled" from each other on a larger scale of length. This can be appreciated if we look at Fig. 3(b), which is a larger version of the previous figure. The red-shaded clusters are distributed along the principal X and Y axes, but are *separated* from each other beyond a certain extent by light red boxes. The black clusters representing amplitude voids are now seen to span larger spatial distances. A similar construction is possible for $ka = -\pi/6$, which is another solution of Eq. (9) for $n = 1$, but this does not have any additional significance. In terms of light, the entire hierarchical geometry will have an appearance where light will be *localized* with higher intensity at certain clusters of waveguides decoupled from each other by completely dark patches.

It is apparent from the above discussion that the eigenfunction corresponding to $ka = \pm\pi/6$ will be localized in the fractal space. This is easily reconfirmed by studying the evolution of the hopping integrals under successive RSRG steps. The hopping integrals t and λ (zero initially, but grows

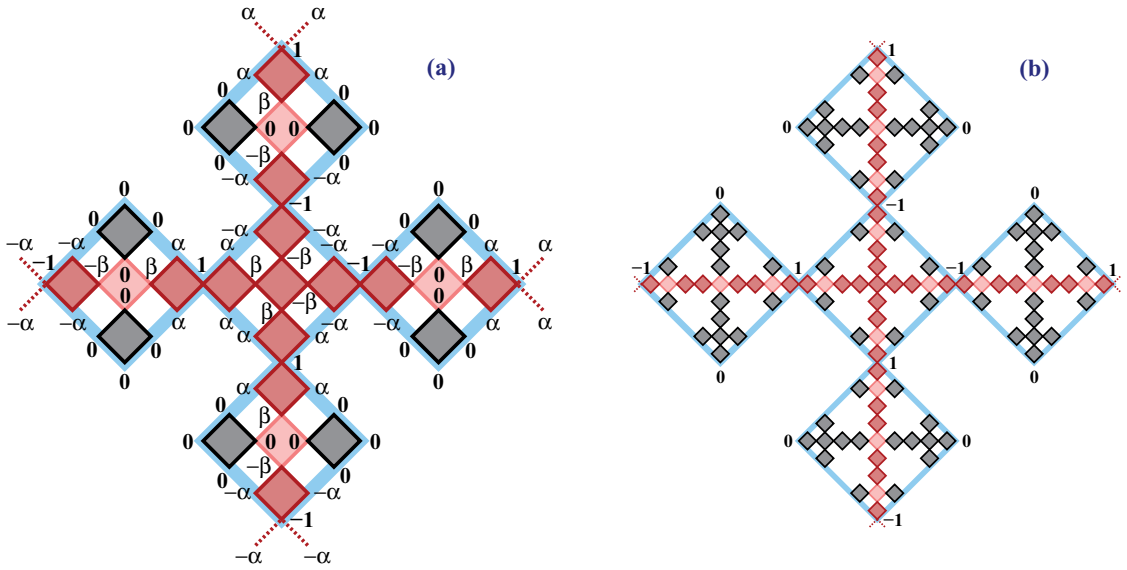

FIG. 3. (Color online) (a) Distribution of amplitudes of the wave function for $ka = \pi/6$ [obtained by solving Eq. (9) for $n = 1$] on a second-generation network. The dark-shaded plaquettes with black lines at the boundary embrace network vertices with zero amplitude. The deep red waveguide segments (covering a dark-red-shaded region) connect vertices with nonzero amplitude and "glow" with maximum intensity. The lighter red lines represent waveguide segments which have an intermediate intensity profile. The amplitudes of the wave are marked by the numbers ± 1, 0, $\pm\alpha$, and $\pm\beta$, respectively, where $\alpha = -\sqrt{3}/2$ and $\beta = 1/2$. (b) The distribution of wave amplitudes for $ka = \pi/6$ on a third-generation network. The thick blue lines represent one- and two-step renormalized lattices in panels (a) and (b), respectively.

later) remain nonzero at the first stage of RSRG (that is, $n = 1$), indicating that the nearest-neighboring sites on a one-step renormalized lattice will have a nonzero overlap of the wave functions. They start decaying for $n > 2$ with the decay in $\lambda(n)$ taking place at a much slower rate compared to $t(n)$. This indicates that over a larger scale of length the corresponding states are *localized*, but the effect is a weak one.

C. The staggering effect

The previous observation immediately leads to an innovative way of exactly determining the wave vectors (wavelengths) corresponding to localized wave functions on such a deterministic geometry at an arbitrary scale of length. We do it using the following method.

We can solve Eq. (9), in principle, to get the desired k values for any n. For example, we have done it explicitly for $n = 2$. The roots are obtained from the equation

$$\cos ka(2\cos 2ka - 1)(\cos 2ka - 2\cos 8ka) = 0 \qquad (11)$$

and are given by $ka = \pm\pi/2, \pm\pi/6, \pm 1.317\,862, \pm 1.008\,990, \pm 0.610\,566$, and $\pm 0.133\,440$. For every such ka value, $\pi - ka$ trivially satisfies Eq. (11) and does not affect the spectrum or the character of the eigenmodes, as already stated in Sec. II A. It is thus enough to stick to the principal values of ka within the interval $[0,\pi]$. In every case, on beginning the RSRG iteration with the wave vector k chosen arbitrarily from the above set, the nearest-neighbor overlap integral t and the diagonal one, viz., λ, remain nonzero *at least up to* that specific nth stage of renormalization. After that, as the RSRG progresses, the hoppings flow to zero with λ dominating over t at every step of renormalization. This implies that for any such k value one can draw a nontrivial distribution of wave amplitudes on the renormalized fractal network. When mapped back onto the original lattice the amplitudes will be found to span clusters of increasing size. The exact size of the spanning clusters will be determined by the value of n. The size, for example, with $n = 2$ exceeds that for $n = 1$.

The spanning clusters finally get decoupled from similar clusters when one looks at the distribution over a large enough network. Speaking in terms of the red- and gray-shaded zones, it should be appreciated that the size of the red zone is much bigger for $n = 2$ compared to the $n = 1$ case. We refer the reader to Ref. [50] for understanding the result.

It is now obvious that higher the value of n, the greater the number of roots of the polynomial equation, Eq. (9), will be. The roots have a nice nesting property. The roots obtained from any $(n-1)$th stage are found included in the solution for the nth stage (see ka values for $n = 2$). The additional roots obtained at the nth level over the existing roots from the $(n-1)$th level keep the overlap integrals nonzero up to that specific nth RSRG step. Beyond this step, the overlap finally starts to weaken in magnitude. This immediately implies that for larger values of n, the clusters of nonzero amplitudes span a wider fractal space, and the localization effect begins much later. That is, the onset of localization can be *delayed in space*, at one's will, by choosing to solve Eq. (9) for larger values of n.

It should also be appreciated that, the larger the value of n is, the roots (ka values) become lower and lower submultiples of π. For extremely large values of n, the localization begins at an enormously large scale of length and extrapolating this idea it is clear that as the roots of the Eq. (9) approach the limit $ka \to 0$, which is equivalent to the limit $\omega \to 0$, the modes practically do not localize, a fact consistent with the idea of

classical wave localization. We can thus induce a staggering effect on the localization of waves in such a fractal waveguide network.

Before we end this subsection, it is pertinent to emphasize that the analysis of the localization of classical waves in this fractal network has been done by exploiting the analogy of the network equations with that of an electron propagating in a similar lattice. This mapping is a mathematical construction and once this is done the RSRG recursion relations are insensitive to whether the input comes from a quantum case or a classical one. However, in the classical case, the material parameters play a crucial role. For example, a given condition on the value of ka implies that the staggering effect can be observed for a special combination of the dielectric condition and the length of the waveguide segment. If we fix the length of the waveguide segment at the very outset, then one can figure out the appropriate wavelengths for which localization will show up at an appropriate length scale, that is, the size of the network itself.

On the other hand, in the electronic case, the wave function amplitude is defined only at the vertices of the diamond plaquettes. The Fermi energy E needs to be tuned to see the staggered localization effect. The numerical values of the lattice constant and the hopping integral at the initial stage are not important as far as the localization is concerned. Also, in the case of localization of classical waves, as already mentioned, there will be a distinct variation of the intensity throughout the fractal network. Each waveguide segment having zero amplitudes at its end will basically sustain a standing wave. The entire segment will have some glow (vertices will be dark though), and this glow will be much less compared to that of the plaquettes where we really have nonzero amplitudes at all the vertices, as depicted schematically in Fig. 3.

D. Transmission of waves

To get the two-terminal conductance for a finite-size diamond-Vicsek fractal, we attach the system between two semi-infinite one-dimensional single-channel waveguides. The wave equation obeyed by the incident wave in these waveguides is discretized, and the leads are artificially converted into arrays of effective *nodes* characterized by a constant on-site potential, $\epsilon_l = 2\cos ka + 2\cot ka$, as before, and a nearest-neighbor overlap integral, $t_l = 1/\sin ka$. We then successively renormalize the finite network to reduce it into an effective two-vertex system, with a renormalized effective on-site term equal to $\mathcal{U}$ and with an effective hopping integral, $\mathcal{T}$, between them. The transmission coefficient across the effective dimer is given by the well-known formula [55]

$$T = \frac{4\sin^2 ka}{\mathcal{D}_1^2 + \mathcal{D}_2^2}, \tag{12}$$

where $\mathcal{D}_1 = [(M_{12} - M_{21}) + (M_{11} - M_{22})\cos ka]$ and $\mathcal{D}_2 = [(M_{11} + M_{22})\sin ka]$. The matrix elements M_{ij} are given by $M_{11} = \frac{(E-\mathcal{U})^2}{\mathcal{T}t_l} - \frac{\mathcal{T}}{t_l}$, $M_{12} = -\frac{(E-\mathcal{U})}{\mathcal{T}}$, $M_{21} = -M_{12}$, $M_{22} = -\frac{t_l}{\mathcal{T}}$, and $\cos ka = (E - \epsilon_l)/2t_l$, with a being the lattice constant and taken to be equal to unity throughout the calculation.

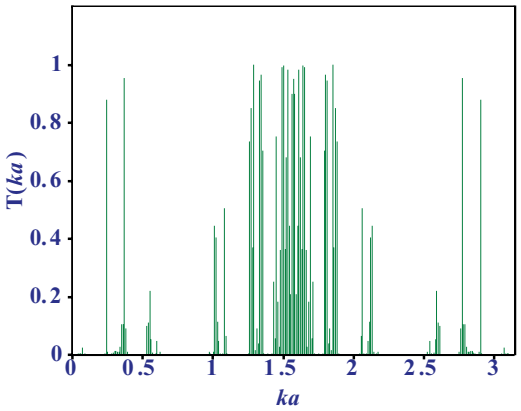

FIG. 4. (Color online) Transmission characteristics for a third-generation Vicsek waveguide network. The length of each monomode segment a is chosen to be unity.

In Fig. 4, we have shown the two-terminal transmission characteristics for a third-generation waveguide network system. The transmission spectrum is, as expected, full of gaps, with resonant transmission exhibited at certain k values. With increasing generation, the resonances become rarer and the spectrum becomes much more fragmented.

IV. CONCLUDING REMARKS

In conclusion, we have examined the distribution of intensity of a classical wave propagating in a Vicsek geometry consisting of diamond-shaped single-channel waveguides. The major result is that we have been able to identify a countable infinity of localized eigenmodes displaying a multitude of localization lengths. A prescription is given for an exact determination of the wave vectors corresponding to all such modes, a problem that is far from trivial in the case of a deterministically disordered system. The localized wave functions span the fractal space in clusters of increasing sizes, the size being precisely controlled by the length scale at which the wave vector (k) is evaluated. The onset of localization can be exactly predicted from the stage of the RSRG and can be delayed (staggered) in space. The study provides a unique opportunity to experimentally examine the localization of classical waves, for example, light, triggered by the lattice topology without bothering about the high dielectric constant materials. It might be useful in developing novel photonic band-gap structures, where the wavelengths to be screened or allowed to go through can be controlled over arbitrarily small domains exploiting the fractal character of the network.

ACKNOWLEDGMENTS

B.P. acknowledges the financial support through an INSPIRE Fellowship from the Department of Science and Technology, India.

[1] P. W. Anderson, Phys. Rev. **109**, 1492 (1958).
[2] E. Abrahams, P. W. Anderson, D. C. Licciardello, and T. V. Ramakrishnan, Phys. Rev. Lett. **42**, 673 (1979).
[3] A. MacKinnon and B. Kramer, Phys. Rev. Lett. **49**, 695 (1982).
[4] D. J. Thouless, Phys. Rev. Lett. **61**, 2141 (1988).
[5] V. Uski, B. Mehlig, and M. Schreiber, Phys. Rev. B **66**, 233104 (2002).
[6] A. Rodriguez, L. J. Vasquez, K. Slevin, and R. A. Römer, Phys. Rev. Lett. **105**, 046403 (2010).
[7] A. Rodriguez, L. J. Vasquez, K. Slevin, and R. A. Römer, Phys. Rev. B **84**, 134209 (2011).
[8] M. Zilly, O. Ujsághy, M. Woelki, and D. E. Wolf, Phys. Rev. B **85**, 075110 (2012).
[9] C. Echeverria-Arrondo and E. Ya. Sherman, Phys. Rev. B **85**, 085430 (2012).
[10] T. A. Sedrakyan, J. P. Kestner, and S. Das Sarma, Phys. Rev. A **84**, 053621 (2011).
[11] E. E. Edwards, M. Beeler, T. Hong, and S. L. Rolston, Phys. Rev. Lett. **101**, 260402 (2008).
[12] G. Roati, C. D'Errico, L. Fallani, M. Fattori, C. Fort, M. Zaccanti, G. Modugno, M. Modugno, and M. Inguscio, Nature (London) **453**, 895 (2008).
[13] U. Gavish and Y. Castin, Phys. Rev. Lett. **95**, 020401 (2005).
[14] J. E. Lye, L. Fallani, M. Modugno, D. S. Wiersma, C. Fort, and M. Inguscio, Phys. Rev. Lett. **95**, 070401 (2005).
[15] J. Billy, V. Josse, Z. Zuo, A. Bernard, B. Hambrecht, P. Lugan, D. Clément, L. Sanchez-Palencia, P. Bouyer, and A. Aspect, Nature (London) **453**, 891 (2008).
[16] S. John, Phys. Rev. Lett. **53**, 2169 (1984).
[17] P. W. Anderson, Philos. Mag. B **52**, 505 (1985).
[18] D. M. Jović, M. R. Belić, and C. Denz, Phys. Rev. A **85**, 031801(R) (2012).
[19] K. Y. Bliokh, S. A. Gredeskul, P. Rajan, I. V. Shadrivov, and Y. S. Kivshar, Phys. Rev. B **85**, 014205 (2012).
[20] D. M. Jović, Y. S. Kivshar, C. Denz, and M. R. Belić, Phys. Rev. A **83**, 033813 (2011).
[21] W. Gellermann, M. Kohmoto, B. Sutherland, and P. C. Taylor, Phys. Rev. Lett. **72**, 633 (1994).
[22] A. A. Asatryan, L. C. Botten, M. A. Byrne, V. D. Freilikher, S. A. Gredeskul, I. V. Shadrivov, R. C. McPhedran, and Y. S. Kivshar, Phys. Rev. B **85**, 045122 (2012).
[23] C. H. Hodges and J. Woodhouse, J. Acoust. Soc. Am. **74**, 894 (1983).
[24] S. He and J. D. Maynard, Phys. Rev. Lett. **57**, 3171 (1986).
[25] E. Yablonovitch and T. J. Gmitter, Phys. Rev. Lett. **63**, 1950 (1989).
[26] Z. Shi and A. Z. Genack, Phys. Rev. Lett. **108**, 043901 (2012).
[27] See, *Photonic Band Gap Materials*, edited by C. M. Soukoulis (Kluwer Academic, Dordrecht, 1995).
[28] S. John, Phys. Rev. Lett. **58**, 2486 (1987).
[29] E. Yablonovitch, Phys. Rev. Lett. **58**, 2059 (1987).
[30] Z. Q. Zhang, C. C. Wong, K. K. Fung, Y. L. Ho, W. L. Chan, S. C. Kan, T. L. Chan, and N. Cheung, Phys. Rev. Lett. **81**, 5540 (1998).
[31] L. Dobrzynski, A. Akjouj, B. Djafari-Rouhani, J. O. Vasseur, and J. Zemmouri, Phys. Rev. B **57**, R9388 (1998).
[32] J. O. Vasseur, B. Djafari-Rouhani, L. Dobrzynski, A. Akjouj, and J. Zemmouri, Phys. Rev. B **59**, 13446 (1999).
[33] R. D. Pradhan and G. H. Watson, Phys. Rev. B **60**, 2410 (1999).
[34] M. Li, Y. Liu, and Z.-Q. Zhang, Phys. Rev. B **61**, 16193 (2000).
[35] S. Sengupta and A. Chakrabarti, Phys. Lett. A **341**, 221 (2005).
[36] S. Sengupta and A. Chakrabarti, Phys. E **28**, 28 (2005).
[37] J. Lu, X. Yang, G. Zhang, and L. Cai, Phys. Lett. A **375**, 3904 (2011).
[38] J. Lu, X. Yang, and L. Cai, Opt. Commun. **285**, 459 (2012).
[39] E. Domany, S. Alexander, D. Bensimon, and L. P. Kadanoff, Phys. Rev. B **28**, 3110 (1983).
[40] R. Rammal, J. Phys. (Paris) **45**, 191 (1984).
[41] P. Kappertz, R. F. S. Andrade, and H. J. Schellnhuber, Phys. Rev. B **49**, 14711 (1994).
[42] W. A. Schwalm and M. K. Schwalm, Phys. Rev. B **47**, 7847 (1993).
[43] A. Chakrabarti and B. Bhattacharyya, Phys. Rev. B **54**, R12625 (1996).
[44] A. Chakraborti, B. Bhattacharyya, and A. Chakrabarti, Phys. Rev. B **61**, 7395 (2000).
[45] X. R. Wang, Phys. Rev. B **51**, 9310 (1995).
[46] A. Chakrabarti, J. Phys.: Condens. Matter **8**, 10951 (1996).
[47] E. Maciá, Phys. Rev. B **57**, 7661 (1998).
[48] W. A. Schwalm and B. J. Moritz, Phys. Rev. B **71**, 134207 (2005).
[49] A. Chakrabarti, Phys. Rev. B **72**, 134207 (2005).
[50] B. Pal and A. Chakrabarti, Phys. Rev. B **85**, 214203 (2012).
[51] T. Vicsek, *Fractal Growth Phenomena*, 2nd ed. (World Scientific, Singapore, 1992).
[52] B. W. Southern, A. A. Kumar, and J. A. Ashraff, Phys. Rev. B **28**, 1785 (1983).
[53] S. Alexander, Phys. Rev. B **27**, 1541 (1983).
[54] Z.-Q. Zhang and P. Sheng, Phys. Rev. B **49**, 83 (1994).
[55] A. D. Stone, J. D. Joannopoulos, and D. J. Chadi, Phys. Rev. B **24**, 5583 (1981).